

Supporting information for

## Humidity-Accelerated Spreading of Ionic Liquids on Mica Surface

Zhantao Wang, Fuxi Shi, Cunlu Zhao\*

\*Corresponding Author: [mclzhao@mail.xjtu.edu.cn](mailto:mclzhao@mail.xjtu.edu.cn) (C. Zhao)

### Supporting Information 1 –

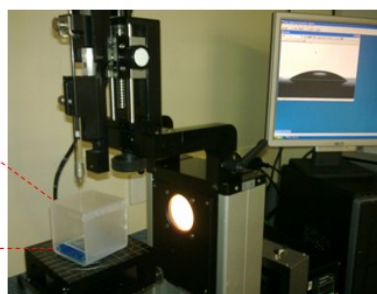
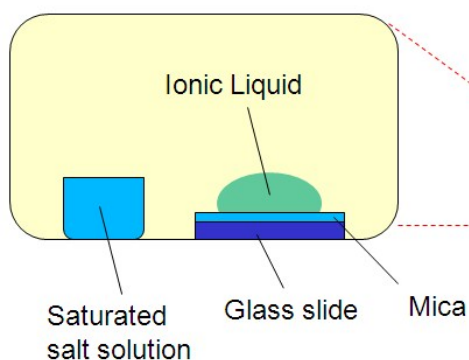
#### Control of relative humidity

A 0.2 L air tight quartz cell was used for the contact angle measurement at different RH (see Figure. S1). Saturated salt solutions were used to maintain the RH inside the cell at various levels (see Table 1)<sup>1</sup>. The relative humidity inside the cell was measured using a calibrated hygrometer. The freshly cleaved mica was placed in the cell together with the salt solution for 6 hours to equilibrate the surface with vapour adsorption. The high purity ( $\geq 99\%$ ) ionic liquid droplets were deposited on the equilibrated mica substrate, and the contact angle relaxation was recorded using the SCA 20 system of Data Physics.

Table 1 Equilibrium relative humidity of selected saturated salt solutions at 23 °C

Salt solution	R.H. % ( $\pm 2$ )	Salt solution	R.H. % ( $\pm 2$ )
Potassium acetate	20	Cobald chloride	65
Magnesium chloride	35	Sodium chloride	75
Potassium carbonate	45	Potassium chloride	85
Magnesium nitrate	55	Potassium sulphate	90

### Controlled Humidity Chamber



### Sessile Drop Method

Figure S1 Humidity control and contact angle measurement

### Supporting Information 2 –

#### Measurement of the advancing and receding contact angles of [bmim][NTf<sub>2</sub>] on freshly cleaved mica at normal ambient humidity of 37%.

The advancing and receding contact angle of [bmim][NTf<sub>2</sub>] on freshly cleaved mica was measured using the SCA 20 of Data Physics. The advancing contact angle was measured by depositing a 2  $\mu\text{L}$  droplet of [bmim][NTf<sub>2</sub>] on freshly cleaved mica and slowly increasing the volume of the droplet using a Hamilton 100  $\mu\text{L}$  syringe, until the apparent triple line starts to advance. The receding contact angle was measured by slowly retracting the liquid from the droplet using the same syringe, until the apparent contact line starts to recede. Each data point was collected by advancing/receding the contact line at different time after deposition of the droplet.

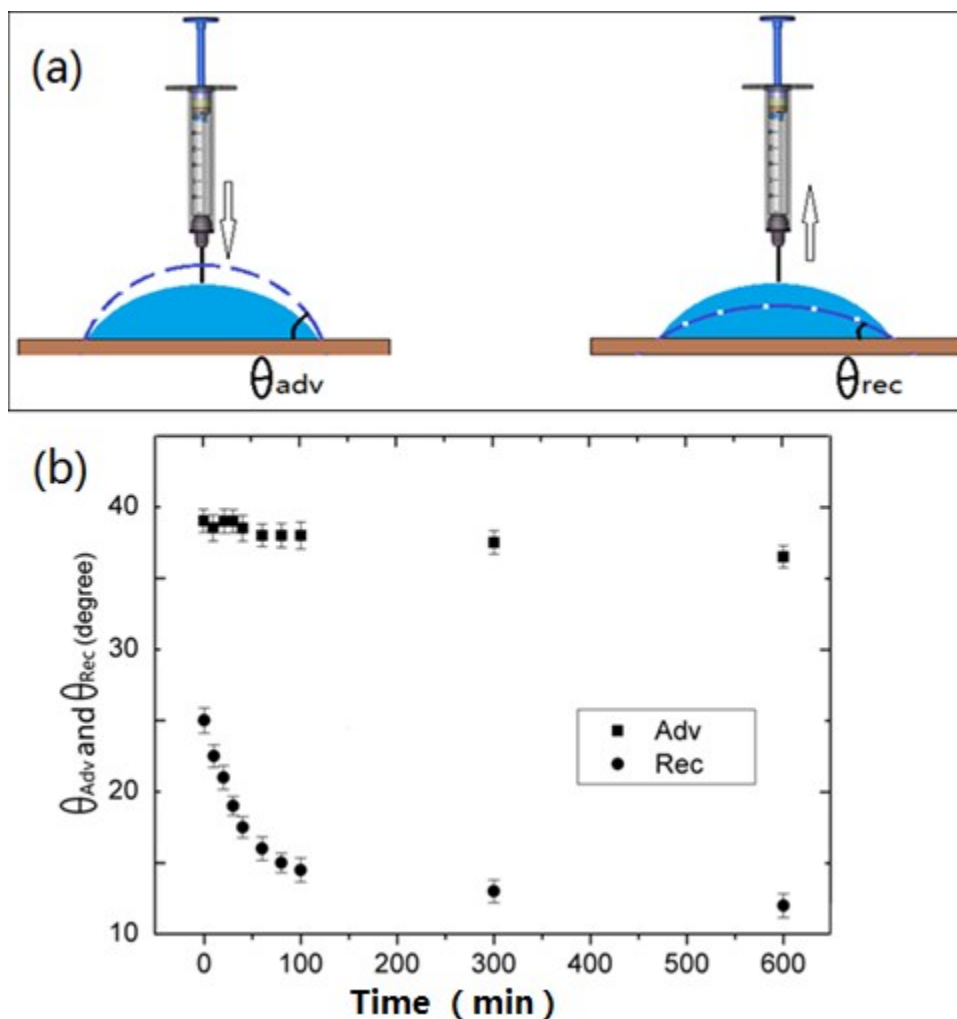


Figure S2 (a). Measurement of contact angle hysteresis against time of [bmim][NTf<sub>2</sub>] on freshly cleaved mica; (b). The corresponding result against time at RH of 37%, where each data point is obtained by advancing and receding the droplet using the syringe.

### Supporting Information 3 –

#### Pre-wetting, AFM imaging and contact angle measurement

The first step, pre-wetting of mica was done by dipping the freshly cleaved mica disk into the pure [bmim][NTf<sub>2</sub>] and taking it out (Figure S3). The second step is tapping mode AFM imaging of the pre-wetted mica disk (Figure S4a) and the third step was measuring the contact angle variation of a droplet deposited on the pre-wetted mica surface, as a function of time (Figure S4b). Figure S4a suggests that the mica surface was covered by a film of ~3 nm thickness, which we interpreted as a monolayer of ion pair of [bmim][NTf<sub>2</sub>]. Figure S4b compares the contact angle of [bmim][NTf<sub>2</sub>] droplet on a freshly cleaved mica with that on a pre-wetted mica by the same IL. The result suggests that the contact angle on a pre-wetted mica surface by the same IL is stable and does not change with time.

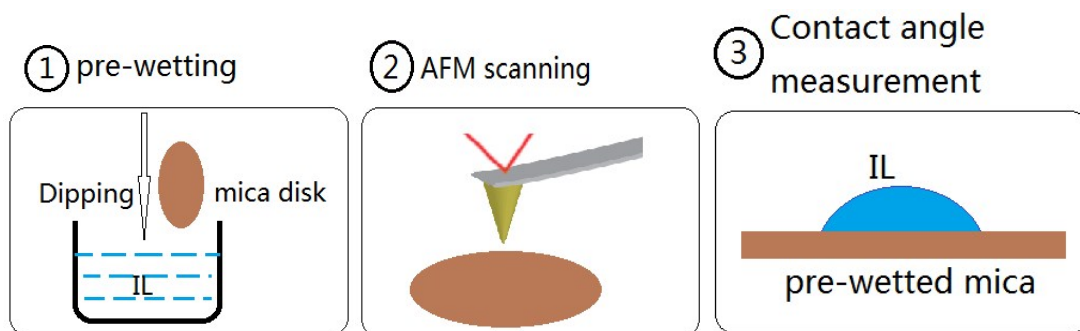


Figure S3 Procedures of pre-wetting experiments and surface characterization

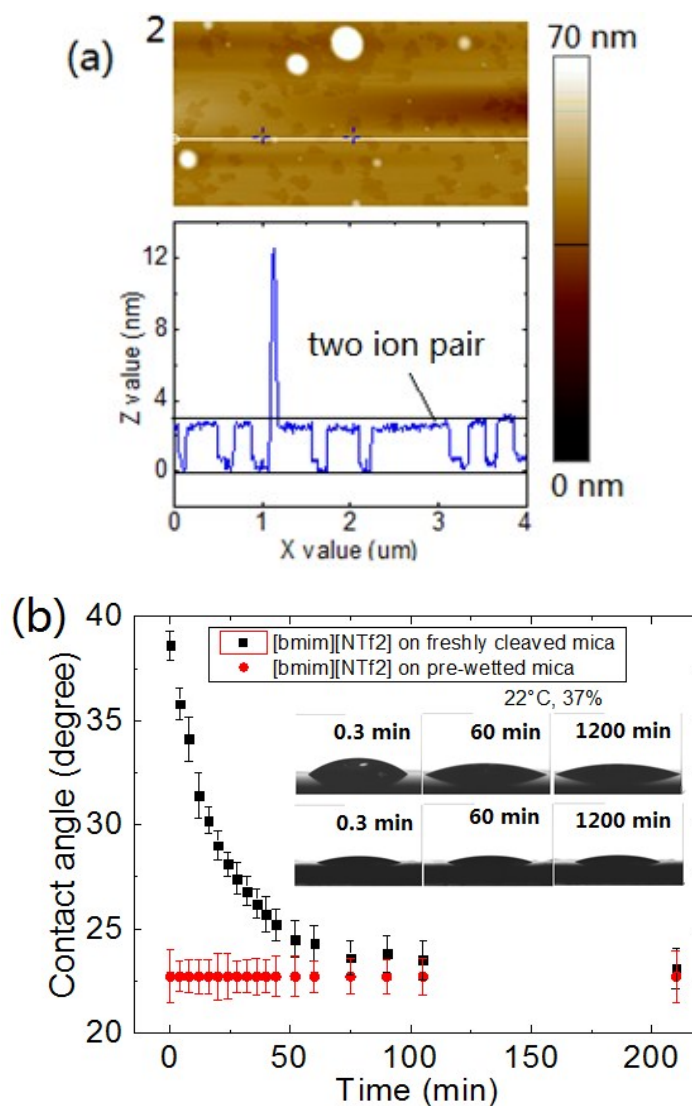


Figure S4 (a). Tapping mode AFM image of a mica surface pre-wetted by [bmim][NTf<sub>2</sub>], scan size is  $4 \mu\text{m} \times 2 \mu\text{m}$ ; (b). Contact angle against time of [bmim][NTf<sub>2</sub>] on the pre-wetted mica surface, the contact angle relaxation of [bmim][NTf<sub>2</sub>] on freshly cleaved mica was also shown as a comparison. The inset images show the droplet profile taken at different time after deposition. Upper inset corresponds to freshly cleaved mica and lower inset corresponds to pre-wetted mica.

## Supporting Information 4 -

### Variation of droplet radius with time

The droplet radius  $R$  (mm) was extracted from the sessile drop images of the spreading droplet. The variation of  $R$  (mm) against the square root of time  $\sqrt{t}$  ( $\sqrt{\text{min}}$ ) was plotted in Figure S5 and fitted to a linear function of  $\sqrt{t}$ . The droplet radii increased approximately linearly with  $\sqrt{t}$  before it levels off, which resembles the spreading behaviour of precursor films through surface diffusion <sup>2</sup>.

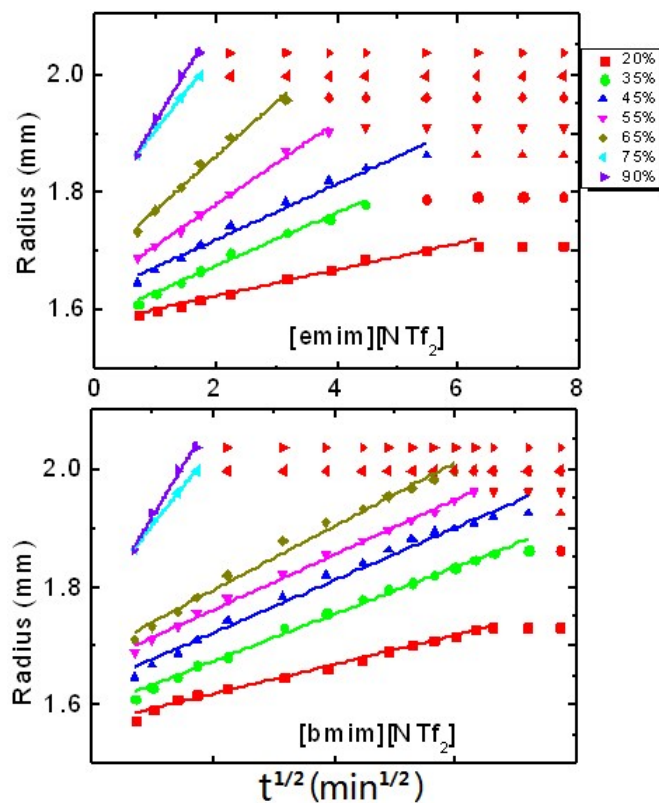


Figure S5 Droplet radius of two ILs as a function of the square root of time: (a) [emim][NTf<sub>2</sub>]; (b) [bmim][NTf<sub>2</sub>].

### References

1. A. Wexler and S. Hasegawa, *J. Res. Natl. Bur. Stand.*, 1954, **53**, 19-26.
2. S. Villette, M. Valignat, A. Cazabat, L. Jullien and F. Tiberg, *Langmuir*, 1996, **12**, 825-830.